

Received March 04, 2020; reviewed; accepted May 11, 2020

Synthesis of a magnetic ionic liquid ([C₁₂mim]FeCl₄) and its interactions with low-rank coal

Zhihao Li¹, Mingpu Liu¹, Mengyu Lin¹, Chuandong Ma¹, Meng He¹, Qingbiao Wang², Hao Yu¹, Lin Li¹, Xiaofang You¹

¹ College of Chemical and Environmental Engineering, Shandong University of Science and Technology, Qingdao 266590, China

² National Engineering Laboratory for Coalmine Backfilling Mining, Shandong University of Science and Technology, Tai'an, Shandong 271019, China

Corresponding author: lilin_1983123@sdust.edu.cn (Lin Li)

Abstract: The large number of oxygen-containing functional groups present on the surface of low-grade coal contribute to its strong hydrophilic properties and rendering coal beneficiation by flotation challenging. In this study, a magnetic ionic liquid (IL), [C₁₂mim]FeCl₄, was developed as a green medium to treat low-rank coal. Notably, the IL can be recovered using a magnetic field. The interactions between the low-rank coal and the IL were analyzed, and the structure and properties of [C₁₂mim]FeCl₄ were characterized using Raman spectroscopy, Fourier-transform infrared (FT-IR) spectroscopy, and vibrating-sample magnetometry. Moreover, the effects of the newly prepared IL on the wetting properties of low-rank coal were studied using water contact angle measurements. The contact angle of the coal sample treated with the IL increased initially but decreased with subsequent increase in treatment time, indicating a change in coal wettability with time. The results from FT-IR analysis show that the changes in contact angles may be attributed to the changes to the oxygen-containing functional groups at the coal surface upon interaction with the IL, where the content of oxygen-containing functional groups in the treated coal sample initially decreased but subsequently increased with increase in treatment time. X-ray photoelectron spectroscopy analysis confirmed these results. Thus, it can be concluded that [C₁₂mim]FeCl₄ initially destroys the oxygen-containing functional groups at the coal surface, resulting in an increase in the water-coal contact angle but subsequently promoting oxidation of the coal surface, hence causing a reduction in the contact angle.

Keywords: low-rank coal, magnetic IL, wettability, contact angle

1. Introduction

Proven reserves of low-rank coal exceed 465 billion tons worldwide, accounting for > 40% of the total proven coal reserves. Moreover, China's proven reserves of low-rank coal exceed 200 billion tons and account for approximately 20% of the proven Chinese coal reserves (Li et al., 2013). Thus, global low-rank coal resources are abundant, but the surface hydrophobicity of this type of coal is poor because of the hydrophilicity of the oxygen-containing functional groups on the coal surface, which complicates the use of this coal (Gutierrez-Rodriguez and Aplan, 1984; Lyu et al., 2018; Zhu et al., 2019). When the oxygen content of the coal surface reaches a certain threshold, it becomes the primary factor determining the surface hydrophobicity. As a result of oxidation, the number of oxygen-containing functional groups on the coal surface increases, readily forming strong hydrogen bonds with water molecules and resulting in a hydration layer on the coal particle surface. This increases the hydrophilicity of the coal sample and reduces its hydrophobicity (W. Zhang et al., 2019). Therefore, to increase the hydrophobicity of low-rank coal, surface modification is necessary to reduce the number of oxygen-containing functional groups, such as hydroxyl, carboxyl, and carbonyl groups (Lan-yun et al., 2011). Several

methods to improve the hydrophobicity of oxidized coal and change the surface properties of low-rank coal have been proposed, although mixed results have been achieved. Using an ionic liquid (IL) for surface modification is a current and environmentally friendly method (Chen et al., 2017; Dey, 2012; Malhotra and Riggs, 1986; Xu et al., 2018; You et al., 2019).

ILs are organic molten salts that remain in the liquid state or close to the liquid state at room temperature; they are composed entirely of anions and cations. ILs have attracted significant attention from both academia and industry as green reaction media, and they have shown great potential for use in various chemical reactions as well as extraction, separation, and material preparation processes (Xiao et al., 2005; Yanget al., 2017). Several studies have reported that ILs can destroy the oxygen-containing functional groups on the surfaces of coal particles. Painter et al. (2010) studied the extent to which ILs can dissolve, shatter, and disperse coal samples. Döbbelin and He (Döbbelin et al., 2010; He et al., 2008) found that polymers containing ILs can be used to prepare surfaces with switchable wettabilities. Dey et al. (Dey, 2012) reported that the unique hydrophilic substructure of various surfactants based on ILs can increase coal wettability via electrostatic and hydrogen-bond-based adsorption after contact with lignite and oxidized coal containing large quantities of oxygen-rich functional groups. Crawford et al. (Crawford & Mainwaring, 2001) suggested that surfactant adsorption on coal surfaces changes its zeta potential and the coal–water contact angle. Using contact angle measurements, Zhang et al. (2018a; 2018b) confirmed that the wettability of ionic-liquid-treated coal was higher than that of coal treated with deionized water. Thus, it is important to explore the effects of ILs as surfactants on coal wetting characteristics. Various reports (Liu et al., 2013; Shi et al., 2002; Zhu, et al., 2019, Zhu et al., 2020) have shown that the structures of ILs can be easily modified, and their physicochemical properties can thus be adjusted as desired. Consequently, they can be used to produce surfactants with the desired degree of hydrophobicity, hydrophilicity, or amphiphilicity, and they represent a potential avenue for changing coal wettability and preventing coal dust generation. Recent reports (Cummings et al., 2015; Pulati et al., 2012; Zhen et al., 2018) have suggested that ILs can change the surface structure of coal significantly. Wang et al. (Wang et al., 2012) used ILs to change the oxidation activity of coal, but few studies have reported the effects of ILs on the coal surface structures. Therefore, it is necessary to explore the relationships between coal wettability and the structural changes caused by ILs to elucidate the underlying microscale mechanisms.

Despite their potential, ILs have a few shortcomings: they are expensive and difficult to recover, which can lead to high costs, poor recyclability, and low applicability. Therefore, effective recycling methods for ILs are urgently needed. As mentioned, a unique feature of ILs is that, by varying the combination of anions and cations, their properties can be adjusted. Thus, ILs are considered “designable solvents” (Liu et al., 2013). Interestingly, magnetic groups can be incorporated into ILs, allowing their recovery by magnetic separation and ensuring their recyclability. In 2004, Hayashi et al. (Hayashi and Hamaguchi, 2005) reported the development of a magnetic IL, 1-methyl-3-butylimidazolium iron(III) tetrachloride ($[\text{C}_4\text{mim}]\text{FeCl}_4$), and Li et al. (X. Li, Yang, Zhou, & Zhang, 2010) synthesized four magnetic alkyl derivatives ($[\text{C}_n\text{mim}]\text{FeCl}_4$; $n = 2, 4, 6, \text{ and } 8$) and three magnetic halide derivatives ($[\text{C}_4\text{mim}]\text{FeX}_4$; $X = \text{Cl, Br}$) of this IL. Chao et al. (Li et al., 2015) used a two-step synthesis process to produce $[\text{C}_4\text{mim}]\text{FeCl}_4$ and $[\text{C}_4\text{mim}]\text{FeBrCl}_3$ magnetic ILs and characterized their structures using Fourier transform infrared (FT-IR) spectroscopy, Raman spectroscopy, and NMR spectroscopy. The biggest advantage of these ILs is their responsiveness to magnetic fields. For example, when used as a reaction medium, the ILs can be recovered and subsequently recycled via magnetic separation, thus greatly improving the efficiency of the process and reducing costs.

In this study, a magnetic IL, 1-methyl-3-dodecylimidazolium iron(III) tetrachloride ($[\text{C}_{12}\text{mim}]\text{FeCl}_4$) was synthesized, and its structure and properties were characterized using Raman spectroscopy, FT-IR spectroscopy, and vibrating-sample magnetometry (VSM). The effects of this magnetic IL on the oxygen-containing functional groups on the surface of coal were investigated using FT-IR spectroscopy and X-ray photoelectron spectroscopy (XPS). The changes in the coal surface wettability were characterized through contact angle experiments, and the underlying mechanism of the interaction of coal with the IL was elucidated.

2. Materials and methods

2.1. Materials

2.1.1. Coal samples

Coal samples from the Daliuta coal mine (Shanxi, China) were selected for the experiment. The coal has the characteristics of low sulfur, low phosphorus and medium to high calorific value. It belongs to long-flame coal and non-bonded coal with high volatile content. Daliuta coal samples were selected for the experiment, because they are low rank coal and they are superficially rich in oxygen-containing functional groups. Coals were dried under vacuum at 60 °C for 24 h. Subsequently, the samples were ground, crushed, and sieved to < 0.074 mm. The results of proximate (moisture, ash, volatile, and fixed carbon (M_{ad} , A_{ad} , V_{daf} , and FC_{daf} , respectively) contents) and ultimate (elemental contents) analyses of the coal samples are shown in Table 1.

Table 1. Industrial of the coal samples

Index	Proximate analysis*/ %				Elemental analysis (daf)/ %				
	M_{ad}	A_{ad}	V_{daf}	FC_{daf}	C	H	N	O	S
Result	5.29	21.60	37.90	62.10	79.50	4.75	0.57	14.21	0.97

* M_{ad} , A_{ad} , V_{daf} , and FC_{daf} indicate the moisture, ash, volatile, and fixed carbon contents, respectively. Subscripts "ad" and "daf" are "air dried" and "dry ash free," respectively.

2.1.2. Preparation of the magnetic IL

A 1:2 molar ratio of $[C_{12}mim]Cl$ IL and $FeCl_3 \cdot 6H_2O$ were placed in a beaker and mixed with a magnetic stirrer for 24 h. Using a desktop high-speed centrifuge, the mixture was centrifuged for 3 min; after 2 h standing, a light green liquid was obtained. The liquid was vacuum dried for 48 h at 80 °C to yield the magnetic IL product: $[C_{12}mim]FeCl_4$.

2.2. Methods

2.2.1. Coal sample treatment

First, 0.50 g of coal was directly mixed with 0.01 mol of $[C_{12}mim]FeCl_4$ in a 10-mL centrifuge tube. The samples were ultrasonicated for 1 min and heated to 30 °C in an oscillator for either 24 or 48 h. The mixture was then filtered through a Büchner funnel and washed with deionized water three times. The filtrate was dried at 105 °C on filter paper for 24 h to obtain the treated coal sample.

2.2.2. Contact angle measurements

The contact angles were measured using a Krüss DSA30 contact angle analyzer. The sessile drop method was used to measure the contact angles on raw and treated coal samples. To achieve this, raw coal and ionic-liquid-treated pulverized coal were cold-extruded into coal samples at 20 MPa. In each contact angle measurement, the same size of deionized (DI) water droplet was used. After the droplet had been placed on the pellet surface and solid-liquid-gas three-phase equilibrium had been reached, an image of the droplet was taken, and contact angle measurement was achieved using the software provided with the instrument. (Arkhipova, 2011) For each coal sample, the contact angle experiment was repeated 15 times under the same experimental conditions, and the arithmetic mean of the test results was taken as the contact angle. By comparing the contact angles between the raw and treated coal samples, the influence of the IL on the coal wetting characteristics was evaluated.

2.2.3. Raman spectroscopy

Raman spectroscopy measurements were carried out with a 300-mW laser in the range of 50–2000 cm^{-1} with a resolution of 4 cm^{-1} . Powdered samples of $[C_{12}mim]FeCl_4$ were prepared and placed on glass sheets for testing.

2.2.4. Fourier transform infrared spectroscopy

The changes in the chemical structure of the coal were studied using ex-situ diffuse reflectance infrared Fourier transform spectroscopy (DRIFTS) (Ma, Wang, Kang, Xin, & Dou, 2019; Qi, Wang, Xin, & Qi, 2014). Before analyzing the coal samples, the KBr background data were collected for baseline reference. The spectra of the samples were recorded from 400 to 4000 cm^{-1} and the average of 64 scans was taken as the final spectrum.

2.2.5. Vibrating-sample magnetometer measurements

VSM (American Quantum Design company, Squid VSM) measurements were carried out. In these measurements, samples were subjected to a magnetic field and magnetized several times while the sample was subjected to strain and the magnetic moment was measured. After measuring the magnetic moment with respect to the magnetic flux density, a hysteresis loop was obtained, and the saturation magnetization intensity, coercivity, and other magnetic parameters were calculated (Sui, Zhang, & Yang, 2018; Zhong, Moore, & Souza).

2.2.6. X-ray photoelectron spectroscopy analysis

X-ray photoelectron spectroscopy (Thermo Scientific ESCALAB 250Xi) was used to analyze the carbon and oxygen contents in the coal samples. The X-ray excitation source was monochromatic Al K_{α} ($h\nu = 1486.6$ eV) with a power of 150 W, X-ray beam spot size of 500 μm , and energy analyzer fixed transmission energy of 30 eV. The adventitious carbon C1s peak was used as the calibration standard. Using the obtained wide and narrow scan spectra, the elemental and functional group compositions were analyzed (Xia & Zhang). Briefly, the XPS peaks of the different elements were fitted and deconvoluted to obtain information concerning the chemical state of the elements on the surface.

3. Results and discussion

3.1. Characterization of the synthesized magnetic IL

3.1.1. Raman spectroscopy

Raman spectroscopy is an effective method for characterizing the organic anions present in an IL, and the spectrum of $[\text{C}_{12}\text{mim}]\text{FeCl}_4$ is shown in Fig. 1. The spectrum of the synthesized IL contains peaks at 120 and 330 cm^{-1} . The peak at 120 cm^{-1} can be assigned to the $[\text{C}_{12}\text{mim}]^+$ cation, whereas that at 330 cm^{-1} can be ascribed to the stretching vibrations of the completely symmetrical Fe-Cl bonds. Thus, these results confirm that the synthesized IL contained $[\text{FeCl}_4]^-$ anions, as expected.

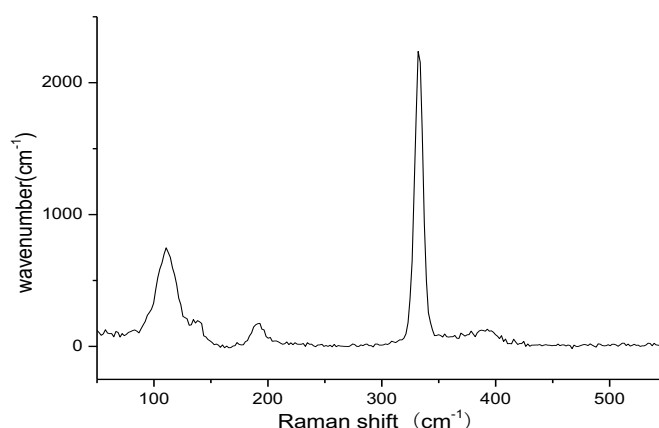


Fig. 1. Raman spectrum of $[\text{C}_{12}\text{mim}]\text{FeCl}_4$

3.1.2. FT-IR analysis

The prepared $[\text{C}_{12}\text{mim}]\text{FeCl}_4$ IL was also characterized by FT-IR spectroscopy, and the results are shown in Fig. 2.

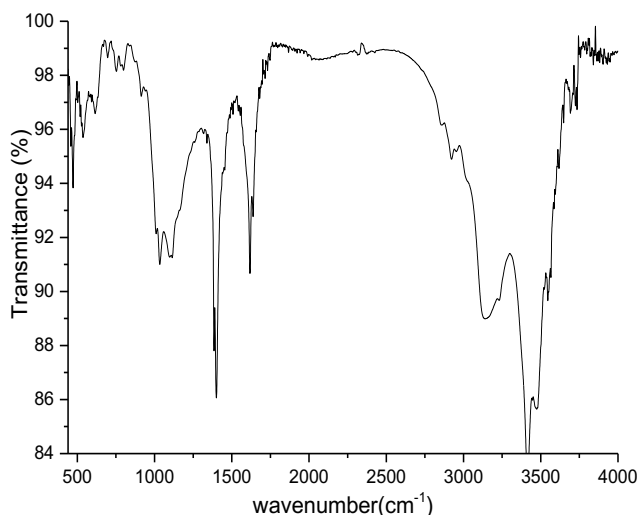


Fig. 2. FT-IR spectrum of $[\text{C}_{12}\text{mim}]\text{FeCl}_4$

The spectrum contains a peak corresponding to the stretching vibrations of the C-H bonds in the aromatic ring at approximately 3150 cm^{-1} , and peaks corresponding to the stretching vibrations of the C-H bonds in the chain at $2850\text{--}2930\text{ cm}^{-1}$. A peak corresponding to the stretching vibrations of the -C=N- group was observed at approximately 1570 cm^{-1} , and another corresponding to the stretching vibrations of the aromatic ring was observed at approximately 1170 cm^{-1} . In addition, peaks arising from the in-plane ring vibrations were observed at $820\text{--}830\text{ cm}^{-1}$, and those corresponding to the out-of-plane ring vibrations were observed at $730\text{--}740\text{ cm}^{-1}$ (Xie and Taubert, 2011; Zhang et al., 2018b).

The cationic structure of the synthesized magnetic IL was consistent with that of the raw material, and no significant differences between the spectra of the two materials was observed, but the spectrum of the magnetic IL exhibited sharper peaks. Therefore, the $[\text{C}_{12}\text{mim}]^+$ cation was not coordinated to the metal center, and only Cl^- and FeCl_3 participated in the complexation reaction. That is, the anion of the complex had little influence on the chemical displacement of the complex. Thus, we determined that the fabricated compound was $[\text{C}_{12}\text{mim}]\text{FeCl}_4$.

3.1.3. VSM measurements and magnetic characterization

The magnetic properties of $[\text{C}_{12}\text{mim}]\text{FeCl}_4$ were analyzed via VSM measurements. The relationship between the magnetization of the IL and strength of the applied magnetic field is shown in Fig. 3.

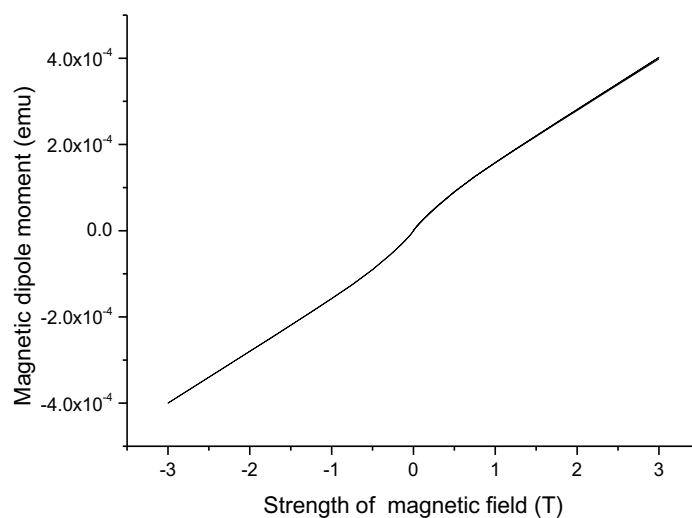


Fig. 3. Relationship between the magnetization of $[\text{C}_{12}\text{mim}]\text{FeCl}_4$ and applied magnetic field strength

From Fig. 3, it is clear that when the magnetic field strength was 0 T, the susceptibility was approximately 0 emu/g, and the magnetic susceptibility of the IL increased almost linearly with increase in magnetic field strength. This suggests that the synthesized magnetic IL was a paramagnetic material, confirming that $[\text{C}_{12}\text{mim}]\text{FeCl}_4$ was indeed magnetic; thus, it might be possible to recycle this material by magnetic separation.

Because ILs usually exist as mixtures with solvents when used as modification reagents, the magnetic behavior of a mixture of $[\text{C}_{12}\text{mim}]\text{FeCl}_4$ with water was studied. A 50% mixture of water and $[\text{C}_{12}\text{mim}]\text{FeCl}_4$ was prepared, yielding two phases. Next, the two-phase mixture was placed in the magnetic field produced by a NdFeB magnet (N50 NdFeB, Sanen Magnetic Industry Co., Ltd., Dongguan). Fig. 4 shows the responses of the mixtures to the external 1.4-T magnetic field. The $[\text{C}_{12}\text{mim}]\text{FeCl}_4$ phase in the mixture moved toward the magnetic pole, indicating that the water and $[\text{C}_{12}\text{mim}]\text{FeCl}_4$ phases can be successfully separated by the application of strong magnetic field (here, 1.4 T).



Fig. 4. Photographs of a 50% v/v mixture of $[\text{C}_{12}\text{mim}]\text{FeCl}_4$ and water in the (a) absence and (b) presence of a 1.4-T magnetic field

3.2. Analysis of coal surface changes induced by IL treatment

3.2.1. Contact angle measurements

Contact angle measurements can be used to analyze coal wettability. The contact angles are listed in Table 2 and photographs of the contact angle measurements are shown in Fig. 5.

As shown by the data in Table 2 and images in Fig. 5, the contact angle increased from 59.32° (untreated) to 94.63° (after 24-h treatment), subsequently decreasing to 77.08° after 48-h treatment. A higher contact angle is indicative of higher hydrophobicity. Based on the measurements, the contact angle of the $[\text{C}_{12}\text{mim}]\text{FeCl}_4$ -treated coal increased after 24-h treatment but decreased after 48-h treatment time, as expected.

Table 2. Results of contact angle measurements

Treatment time, h	Untreated	24	48
Contact angle, $^\circ$	59.32 ± 1.2	94.63 ± 1.8	77.08 ± 1.1
Relative error, %	2.4	3.4	1.9

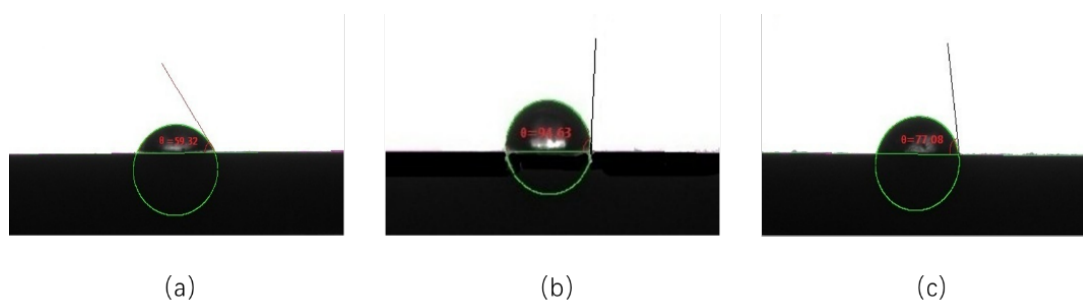


Fig. 5. Contact angles of the (a) untreated coal and those treated with the IL for (b) 24 and (c) 48 h

3.2.2. FT-IR analysis

FT-IR analysis is widely used to analyze the functional groups on coal particle surfaces (Weiqing Zhang, Jiang, Wu, et al., 2018). The results reveal that the coal surface was mainly composed of aliphatic hydrocarbons, aromatic hydrocarbons, oxygen-containing functional groups, and inorganic mineral groups. The carboxyl, hydroxyl, carbonyl, and other oxygen-containing functional groups, along with mineral groups, have the most significant influence on coal hydrophilicity.

Fig. 6 shows that the untreated and treated coal samples contained similar functional groups. Further, the bands corresponding to various functional groups remained largely unchanged after the IL treatment, indicating that the basic framework and structural units of the pulverized and treated coal samples were similar. However, the intensities of some of the peaks were significantly different, likely because of the destruction of some of the functional groups by $[\text{C}_{12}\text{mim}]\text{FeCl}_4$. The IL treatment had a strong effect on the swelling of the coal, thereby destroying the hydroxyl formed in the coal bonds. Based on the literature, the FT-IR peaks that change the most after IL treatment are those arising from oxygen-containing functional groups. The peak intensities of the oxygen-containing functional groups for the coal samples treated with $[\text{C}_{12}\text{mim}]\text{FeCl}_4$ were lower than the corresponding peaks of the untreated coal sample, indicating that some of the oxygen-containing functional groups had been destroyed. Thus, together with the contact angle results, the FT-IR results indicate that the wettability of the coal varied with changes in the content of oxygen-containing functional groups.

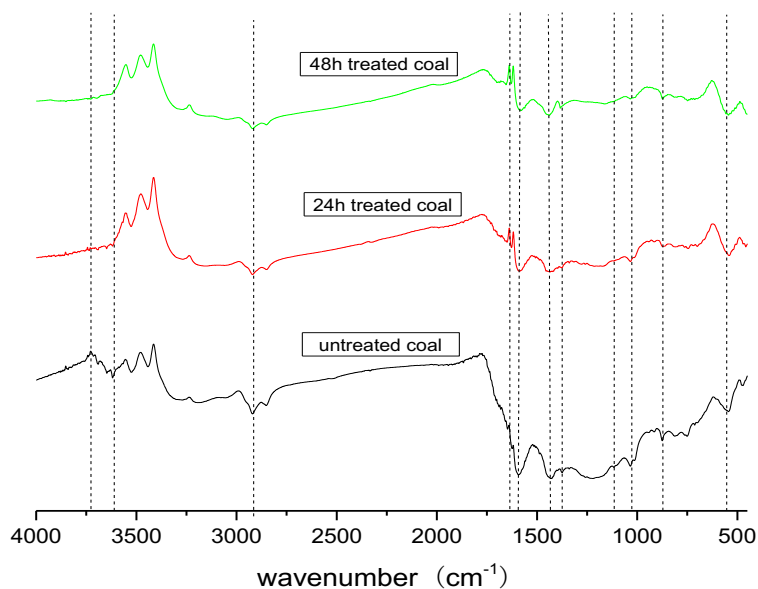


Fig. 6. FT-IR spectra of untreated and IL-treated coal samples

Based on the FT-IR data obtained, the following conclusions can be drawn:

(1) Hydroxyl groups: The band corresponding to free -OH groups in the untreated coal sample was observed at approximately 3750 cm^{-1} . However, this peak disappeared after treatment with the IL for 24 and 48 h, indicating that the free -OH groups had been affected by $[\text{C}_{12}\text{mim}]\text{FeCl}_4$. The peaks at 3620 and 1020 cm^{-1} can be attributed to the stretching vibrations of the phenol hydroxyl group ($\text{C}_6\text{H}_5\text{-OH}$). The relative -OH group content was reduced significantly after treatment for 24 and 48 h, indicating that the two types of hydroxyl functional groups were partially dissolved by $[\text{C}_{12}\text{mim}]\text{FeCl}_4$. The peak at 1120 cm^{-1} in the spectrum of the untreated coal sample, which was attributed to the stretching vibrations of ether bonds, was absent from the spectra of the treated samples (24 and 48 h), indicating that the ether bonds were also affected by $[\text{C}_{12}\text{mim}]\text{FeCl}_4$.

(2) Carbonyl groups: No peaks related to the stretching vibrations of the $\text{C}=\text{O}$ carbonyl group were observed in the spectrum of the untreated coal sample. However, a related peak was observed at approximately 1682 cm^{-1} in the spectra of both treated samples, indicating that carbonyl groups had formed on the coal surface by the action of $[\text{C}_{12}\text{mim}]\text{FeCl}_4$ and water. The peak at 1377 cm^{-1} was

attributed to the stretching vibrations of the carbonyl group (CH₂-C=O) and was observed in the spectra of all three samples. However, the carbonyl peak intensities in the spectra of the untreated and 48-h treated samples were higher than those in the spectrum of the 24-h treated sample, indicating that carbonyl groups were present.

(3) Carboxyl groups: The peak at approximately 1426 cm⁻¹, which was observed in the spectra of all samples, was attributed to the stretching vibrations of COOH. The carboxyl peak intensities in the spectra of the untreated and 48-h-treated samples were higher than those in the spectrum of the 24-h-treated sample, indicating that the carboxyl groups were initially destroyed and subsequently re-formed under the action of [C₁₂mim]FeCl₄ and water.

In general, after treatment with [C₁₂mim]FeCl₄, the hydroxyl, carboxyl, and carbonyl group contents changed, and the FT-IR intensities of the bands associated with hydrogen bonding were weakened or removed. After IL treatment, significant swelling was observed on the coal surface. When solvents are used to disrupt the hydrogen bonding network in coal, the structure of coal is stressed, resulting in swelling and fragmentation. Thus, the FT-IR results indicate that IL treatment resulted in the breakage of the hydrogen-bonding network present in coals. Although FT-IR is suitable for the qualitative analysis of the oxygen-containing functional groups in coal after IL treatment, it does not allow for quantitative analysis. Hence, XPS analysis was also performed.

3.2.3. XPS analysis

XPS analysis was performed to measure the changes in the organic oxygen-containing functional group contents of the coal samples after treatment quantitatively to understand the effects of [C₁₂mim]FeCl₄ on these functional groups. Most oxygen-containing functional groups in coal are composed of O and C. Thus, the chemical environment of the C atoms is influenced by the neighboring O atoms. Thus, narrow XPS scans for C were obtained.

Table 3. Analysis of the narrow-scan C1s XPS data

Group	Untreated		24 h		48 h	
	BE, eV	%	BE, eV	%	BE, eV	%
C-C/C-H	284.75	71.71	284.75	72.54	284.75	72.35
C-O	286.05	16.86	286.05	15.53	286.05	16.77
C=O	287.58	1.71	287.75	6.49	287.75	4.86
O=C-O	289.1	9.72	289.1	5.44	288.48	6.02

The C in coal mainly exists in the form of -C-C-/-C-H-, but it also contains oxygen-containing functional groups, such as -C-O-, -C=O-, and -COO- (X. Liu, Liu, Fan, Guo, & Li; Pietrzak & Wachowska, 2006). The binding energies of the peaks corresponding to the various groups were as follows: -C-C-/-C-H- (284.75 eV), -C-O- (286.05 eV), -C=O- (287.58 eV), and -O=C-O- (289.1 eV). Fig. 7 shows the narrow-scan XPS C1s spectra of the untreated coal and those of the coal samples treated with [C₁₂mim]FeCl₄ for 24 and 48 h. By fitting the XPS peaks of the various samples, the -C-C-/-C-H-, -C-O-, -C=O-, and COO- contents and the positions of their corresponding peaks were determined (Table 3).

Clearly, most of the C in the coal samples was in the form of -C-C-/-C-H-, followed by -C-O-, -C=O-, and COO-. The -C-O- content in the untreated coal sample was 16.86%, but after 24-h treatment with [C₁₂mim]FeCl₄, the content decreased to 15.53%. In contrast, after IL treatment for 48 h, the -C-O- content increased to 16.77%. The COO- content decreased from 9.72% in the untreated coal sample to 5.44% in 24 h-treated sample and subsequently increased to 6.02% in the 48-h-treated sample. This indicates that [C₁₂mim]FeCl₄ had an initial destructive effect on the -C-O- and COO- groups in coal after 24 h, but it promoted the formation of these bonds after 48-h treatment. However, the -C=O- content increased from 1.71% in the untreated sample to 6.49% after 24-h treatment and subsequently decreased to 4.86% after 48-h treatment. From the data, it appears that the -C=O- contents increased. Actually, the -C=O- contents decreased. Because of the low content, the -C-O- and -COO- groups on the coal surface dominate, so the relative content shows an increase of 24 h. The same is true after 48 h, where the relative content of -C=O- is reduced.

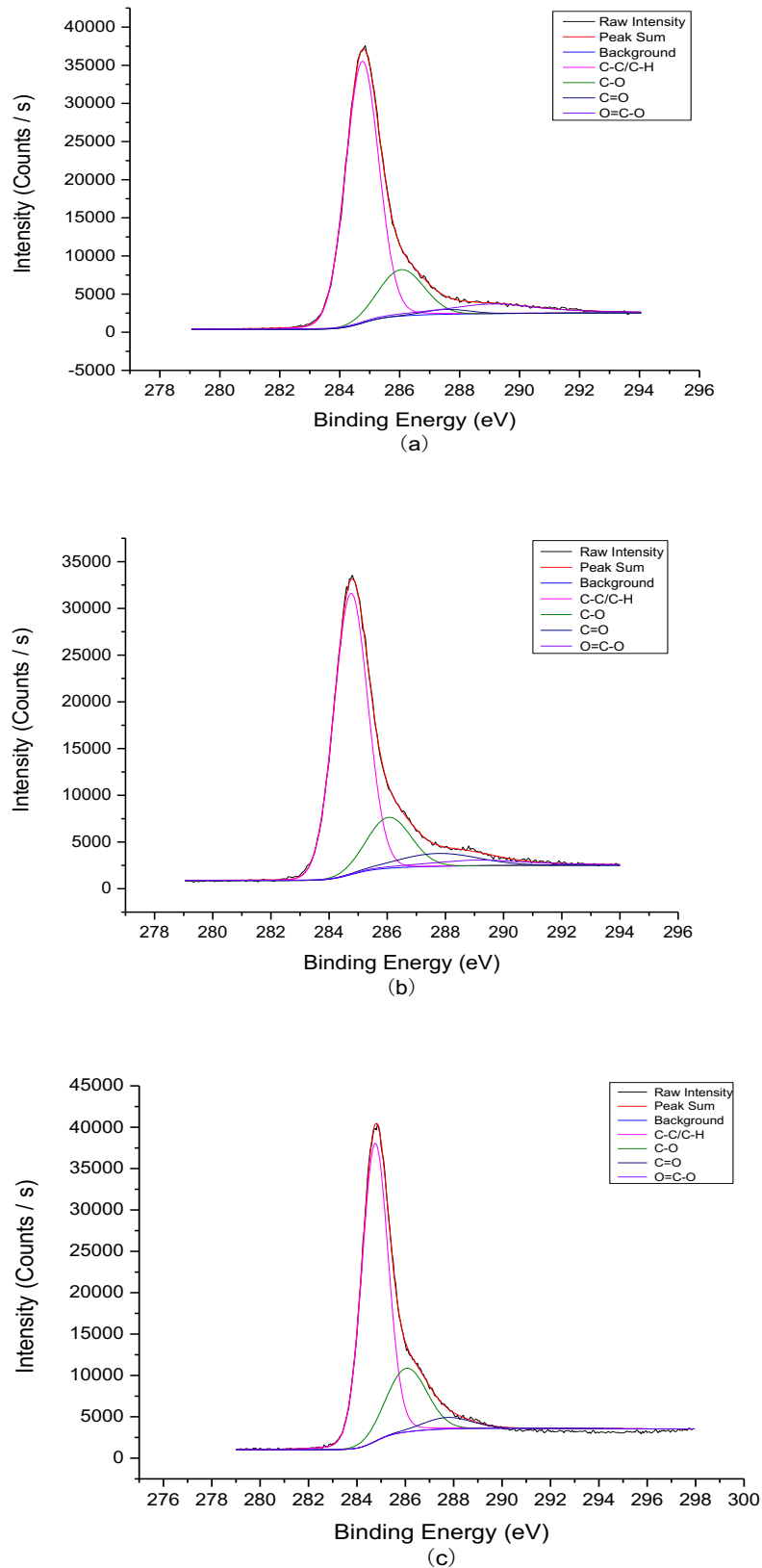


Fig. 7. Narrow-scan C_{1s} spectra of the (a) untreated and (b) 24 and (c) 48-h treated coal samples

The O on the coal surface was mainly present as -C-O- groups, but there were also small amounts of -C=O- and COO-. The binding energies of the peaks related to O in the coal sample were as follows:

C=O- at 531.56 eV, -C-O- at 532.7 eV, and -O=C-O- at 533.93 eV, whereas that of adsorbed oxygen was observed at 535.84 eV (Cai and Zhang, 2013; Present, 2015).

Fig. 8 shows the XPS O1s spectra of the untreated, 24-h-treated, and 48-h-treated coal samples. By fitting the XPS peaks, the peak binding energies of the -C=O-, -C-O-, and COO- groups and the adsorbed oxygen, as well as their contents, were determined (Table 4).

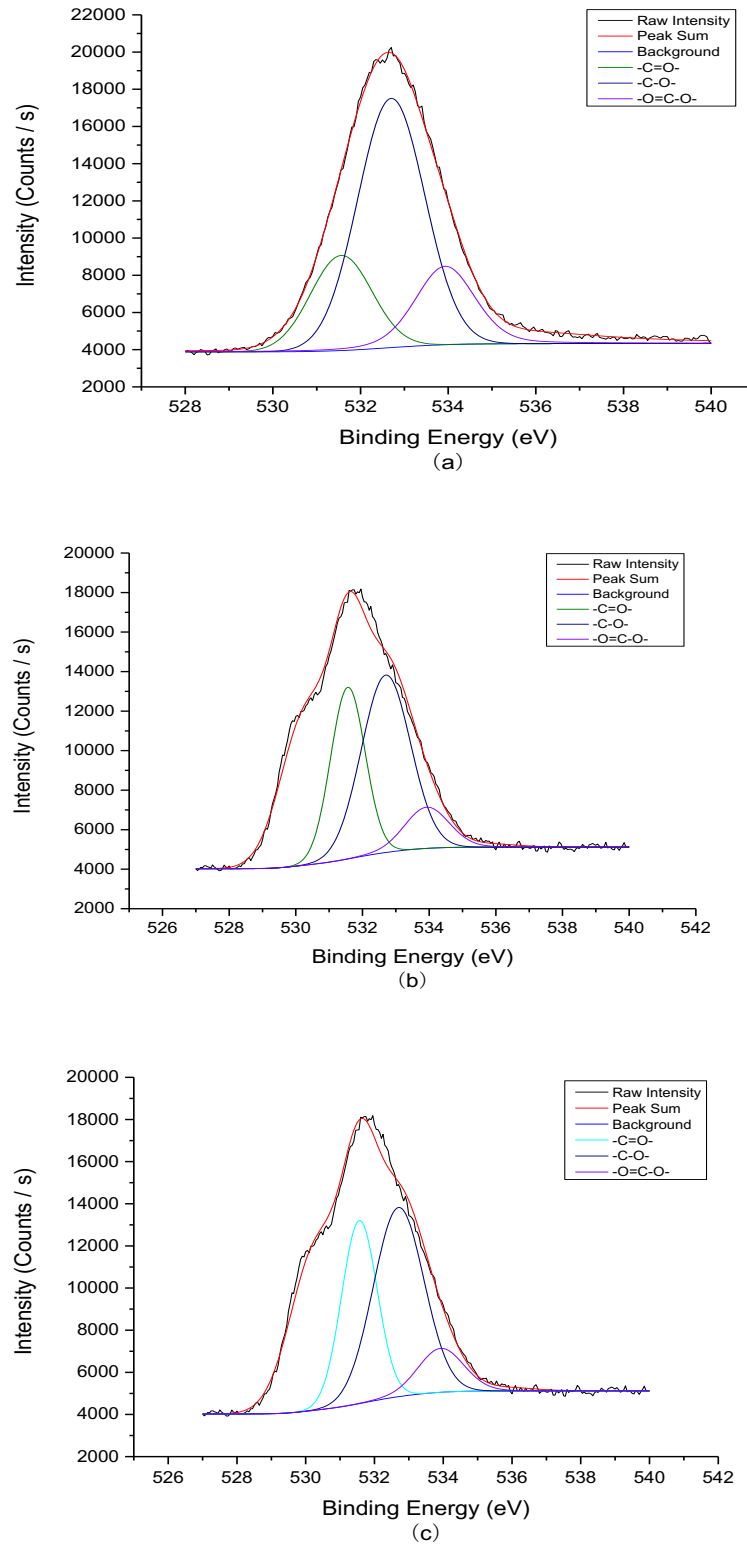


Fig. 8. Narrow-scan O1s spectra of the (a) untreated coal and (b) 24 and (c) 48-h treated coal samples

Table 4. Analysis of the narrow-scan O1s XPS data

Group	Untreated		24 h		48 h	
	BE, eV	%	BE, eV	%	BE, eV	%
-C=O-	531.56	11.04	531.56	25.95	531.56	16.58
-C-O-	532.7	60.33	532.7	52.64	532.7	55.92
-O-C=O-	533.93	28.63	533.93	21.41	533.93	27.50

From the data in Table 4, most of the O in the coal sample existed in the form of -C-O-, followed by -C=O- and COO-. The -C-O- content in the untreated coal sample was 60.33%; after the 24-h treatment with [C₁₂mim]FeCl₄, this content decreased to 52.64%. Furthermore, after 48 h, the -C-O- content again increased to 55.92%, indicating that [C₁₂mim]FeCl₄ had a negative effect on the -C-O- content in coal after 24-h treatment. However, after 48-h treatment, the IL promoted the formation of -C-O- groups. Meanwhile, the COO- content decreased from 28.63% for the untreated sample to 21.41% in the 24 h-treated sample, subsequently increasing to 27.50% in the 48 h-treated sample. This suggests that the IL initially destroyed the COO- groups in the coal but subsequently promoted COO- generation until 48 h. In contrast, the -C=O- content increased from 11.04% initially to 25.95% after 24 h, finally decreasing to 16.58% after 48 h. From the data, it appears that the -C=O- content increased. Actually, the -C=O- content decreased. Because of its low content, the -C-O- and COO- on the coal surface dominate, so the relative content shows an increase after 24 h. The same is true after 48-h treatment, where the relative -C=O- content shows a reduction. These results are consistent with those obtained from the narrow-scan XPS C1s spectral analysis.

4. Conclusions

In this study, a magnetic IL, [C₁₂mim]FeCl₄, was synthesized and the relationship between coal wettability and microstructure after treatment with the magnetic IL were studied. The main conclusions can be summarized as follows:

(1) The magnetic IL [C₁₂mim]FeCl₄ was successfully synthesized, and its anionic and cationic structures were verified by FT-IR and Raman spectroscopy, respectively. This proved that the synthesized magnetic IL was indeed [C₁₂mim]FeCl₄. Furthermore, VSM measurements confirmed that the prepared liquid was paramagnetic.

(2) After treatment with [C₁₂mim]FeCl₄, the coal microstructure changed significantly, primarily in terms of the oxygen-containing functional group content. The contact angle of the treated coal sample differed significantly from that of the untreated sample: increasing initially and then decreasing with increase in treatment time. FT-IR and XPS analyses showed that the IL treatment of the coal for different durations affected the content of hydrophilic oxygen-containing functional groups. The oxygen-containing functional groups on the coal surface were first destroyed by the IL and subsequently regenerated with increasing treatment time. The decreased number of oxygen-containing functional groups on the coal surface improved its hydrophobicity.

Acknowledgements

This work was supported by SDUST Research Fund (Grant No. 2018TDJH101), Key Research and Development Project of Shandong (Grant No. 2019GGX103035), National Natural Science Foundation of China (Grant No. 51904174), Young Science and Technology Innovation Program of Shandong Province (Grant No. 2020KJD001), and Project of Shandong Province Higher Educational Young Innovative Talent Introduction and Cultivation Team.

References

- CAI, C. C., ZHANG, M. X. (2013). *XPS Analysis of Carbon and Oxygen in Coking Coal with Different Density Intervals*. Applied Mechanics & Materials, 347-350, 1239-1243.
- CHEN, Y., XU, G., ALBIJANIC, B. (2017). *Evaluation of SDBS surfactant on coal wetting performance with static methods: Preliminary laboratory tests*. Energy Sources Part A Recovery Utilization & Environmental Effects, 39(3), 1-11.

- CRAWFORD, R.J., MAINWARING, D.E. (2001). *The influence of surfactant adsorption on the surface characterisation of Australian coals*. Fuel, 80(3), 313-320.
- CUMMINGS, J., SHAH, K., ATKON, R., MOGHTADERI, B. (2015). *Physicochemical interactions of ionic liquids with coal; the viability of ionic liquids for pre-treatments in coal liquefaction*. Fuel, 143, 244-252.
- DEY, S. (2012). *Enhancement in hydrophobicity of low rank coal by surfactants – A critical overview*. Fuel Processing Technology, 94(1), 151-158.
- DOBDELIN, M., TENA-ZAERA, R., MARCILLA, R., ITURRI, J., MOYA, S., POMPOSO, J.A., MECERREYES, D. (2010). *Multiresponsive PEDOT-Ionic Liquid Materials for the Design of Surfaces with Switchable Wettability*. Advanced Functional Materials, 19(20), 3326-3333.
- GUTIERREZ-RODRIGUEZ, J.A., APLAN, F.F. (1984). *The effect of oxygen on the hydrophobicity and floatability of coal*. Colloids & Surfaces, 12(1), 27-51.
- HAYASHI, S., HAMAGUCHI, H.O. (2005). *Discovery of a Magnetic Ionic Liquid [bmim]FeCl₄*. Cheminform, 36(18), 1590-1591.
- HE, X., WU, Y., PEI, X. (2008). *Preparation, Characterization, and Tunable Wettability of Poly(ionic liquid) Brushes via Surface-Initiated Atom Transfer Radical Polymerization*. Macromolecules, 41(13), 4615-4621.
- LAN-YUN, W., SHU-GUANG, J., YONG-LIANG, X., WEI-QING, Z., WEN, K.L., ZHENG-YAN, W., TING-XIANG, C. (2011). *Effect of Imidazolium Based Ionic Liquids on Coal Exothermic Oxidation by Thermal Analysis Experiments*. Procedia Engineering, 26, 647-651.
- LI, C., HUANG, Y., HUANG, H. (2015). *Preparation and properties of magnetic ionic liquid*. Journal of Northwest Polytechnic University(1), 76-80.
- LI, X., YANG, F., ZHOU, Q., ZHANG, S. (2010). *Synthesis and characterization of magnetic ionic liquid 1-methyl-3-alkyl imidazole tetrahalide iron salt*. Chinese journal of process engineering, 10(4), 788-794.
- LI, Z., YU, W., YANG, C., ZHOU, A. (2013). *Present situation and prospect of low rank coal quality improvement*. Mining Machinery, 41(7), 1-6.
- LIU, G., GU, D., LIU, H., GU, S. (2013). *Synthesis of ionic liquid bisimidazole surfactant*. Journal of Harbin Institute of Technology, 45(7), 72-78.
- LIU, X., LIU, S., FAN, M., GUO, J., LI, B. (2018). *Decrease in hydrophilicity and moisture readsorption of Manglai lignite using lauryl polyoxyethylene ether: Effects of the HLB and coverage on functional groups and pores*. Fuel Processing Technology, 174, 33-40.
- LYU, X., YOU, X., HE, M., ZHANG, W., WEI, H., LI, L., HE, Q. (2018). *Adsorption and molecular dynamics simulations of nonionic surfactant on the low rank coal surface*. Fuel, 211, 529-534.
- MA, L., WANG, D., KANG, W., XIN, H., DOU, G. (2019). *Comparison of the staged inhibitory effects of two ionic liquids on spontaneous combustion of coal based on in situ FTIR and micro-calorimetric kinetic analyses*. Process Safety & Environmental Protection.
- MALHORTA, D., RIGGS, W.F. (1986). *Chemical reagents in the mineral processing industry*.
- PAINTER, P., PULATI, N., CETINER, R., SOBKOWIAK, M., MITCHELL, G., MATHEWS, J. (2010). *Dissolution and Dispersion of Coal in Ionic Liquids*. Energy & Fuels, 24(3), 1848-1853.
- PIETRZAK, R., WACHOWSKA, H. (2006). *The influence of oxidation with HNO₃ on the surface composition of high-sulphur coals: XPS study*. Fuel Processing Technology, 87(11), 1021-1029.
- PRESENT, A. (2015). *Effects of Oxygen Element and Oxygen-Containing Functional Groups on Surface Wettability of Coal Dust with Various Metamorphic Degrees Based on XPS Experiment*. Journal of Analytical Methods in Chemistry, 2015(1), 467242.
- PULATI, N., SOBKOWIAK, M., MATHEWS, J. P., PAINTER, P. (2012). *Low temperature treatment of Illinois No. 6 coal in ionic liquids*. Energy Fuels, 26(6), 3548-3552.
- QI, X., WANG, D., XIN, H., QI, G. (2014). *An In Situ Testing Method for Analyzing the Changes of Active Groups in Coal Oxidation at Low Temperatures*. Spectroscopy Letters, 47(7), 495-503.
- SHI, J., SUN, X., YANG, C., GAO, Q., LI, Y. (2002). *Research progress of ionic liquid*. chemical bulletin, 65(4), 243-250.
- SUI, W., ZHANG, X., YANG, D. (2018). *How to Measure the Magnetic Characteristics with Vibrating Sample Magnetometer*. Experiment Science & Technology.
- ARKHIPOV, V.A., PALEEY, D. Y., PATARKOV, Y.F., USANINA, A.S. (2011). *Determination of contact angle on the coal surface*. Journal of Mining Science, 47(5), 561-565.
- WANG, L., XU, Y., JIANG, S., YU, M., CHU, T., ZHANG, W., WU, Z.Y., KOU, L. (2012). *Imidazolium based ionic liquids affecting functional groups and oxidation properties of bituminous coal*. Safety Science, 50(7), 1528-1534.

- XIA, W., ZHANG, W. *Characterization of surface properties of Inner Mongolia coal using FTIR and XPS*. Energy Sources Part A Recovery Utilization & Environmental Effects, 39(7-12), 1191-1195.
- XIAO, X., LIU, S., LIU, X., JIANG, S. (2005). *Progress of ionic liquid and its application in separation and analysis*. Analytical Chemistry, 33(4), 569-574.
- XIE, Z. L., TAUBERT, A. (2011). *Thermomorphic Behavior of the Ionic Liquids [C4mim][FeCl4] and [C12mim][FeCl4]*. Chemphyschem, 12(2), 364-368.
- XU, G., CHEN, Y., EKSTEEN, J., XU, J. (2018). *Surfactant-aided coal dust suppression: A review of evaluation methods and influencing factors*. Science of the Total Environment, 639, 1060.
- YANG, X., ZHANG, Y., ZHOU, W., LI, Y., WANG, J. (2017). *Synthesis and applications of ionic liquid surfactant (XII), microemulsion*. Daily Chemical Industry, 47(12), 668-672.
- YOU, X., HE, M., CAO, X., WANG, P., WANG, J., LI, L. (2019). *Molecular dynamics simulations of removal of nonylphenol pollutants by graphene oxide: Experimental study and modelling*. Applied Surface Science, 475, 621-626.
- YOU, X., HE, M., ZHU, X., WEI, H., CAO, X., WANG, P., LI, L. (2019). *Influence of surfactant for improving dewatering of brown coal: A comparative experimental and MD simulation study*. Separation and Purification Technology, 210, 473-478.
- ZHANG, W., JIANG, S., QIN, T., SUN, J., DONG, C., HU, Q. (2019). *Effect of Ionic Liquid Surfactants on Coal Oxidation and Structure*. J. Anal. Methods Chem., 1868265.
- ZHANG, W., JIANG, S., SUN, J., WU, Z., TONG, Q., XIAN, X. (2018). *Wettability of coal by room temperature ionic liquids*. International Journal of Coal Preparation & Utilization(1), 1-10.
- ZHANG, W., JIANG, S., WU, Z., WANG, K., SHAO, H., QIN, T., XI, X., TIAN, H. (2018). *Influence of imidazolium-based ionic liquids on coal oxidation*. Fuel, 217, 529-535.
- ZHEN, L., HE, Y., WANG, W., CHENG, W., LIN, X. (2018). *Experimental Study on the Pore Structure Fractals and Seepage Characteristics of a Coal Sample Around a Borehole in Coal Seam Water Infusion*. Transport in Porous Media, 125(1-2), 1-21.
- ZHONG, S., MOORE, J. E., SOUZA, I. *Gyrotropic Magnetic Effect and the Magnetic Moment on the Fermi Surface*. Physical Review Letters, 116(7), 077201.
- ZHU, X., HE, M., ZHANG, W., WEI, H., LYU, X., WANG, Q., YOU, X., LI, L. (2020). *Formulation design of microemulsion collector based on gemini surfactant in coal flotation*. Journal of Cleaner Production, 120496.
- ZHU, X., WEI, H., HOU, M., WANG, Q., YOU, X., LI, L. (2019). *Thermodynamic behavior and flotation kinetics of an ionic liquid microemulsion collector for coal flotation*. Fuel, 116627.